Available online at www.sciencedirect.com

Chemical Physics Letters ??? (2013) 1–8

CHEMICAL PHYSICS LETTERS

www.elsevier.com/locate/cplett

Rotational structure of the five lowest frequency fundamental vibrational states of dimethylsulfoxide

Arnaud Cuisset*, Marie-Aline Martin Drumel, Francis Hindle, Gaël Mouret, Dmitrií A. Sadovskií

Laboratoire de Physico-Chimie de l'Atmosphère, Maison de la Recherche en Environnement Industriel, Université du Littoral – Côte d'Opale, 59140 Dunkerque, France

Abstract

We report on the successful extended analysis of the high-frequency (200-700 GHz) part of the gas phase (sub)mm-wave spectra of dimethylsulfoxide (DMSO). The spectrum was recorded at 100 kHz resolution using a solid state subTHz spectrometer. The five low frequency fundamental vibrational states of DMSO were observed as sidebands along with the main $0 \leftarrow 0$ band. Neglecting the internal rotation of methyls, our rotational Hamiltonian reproduced the spectrum to the subMHz accuracy. We have found that the asymmetric bending state ν_{23} is the only low frequency fundamental vibrational state with the "anomalous" rotational structure uncovered in [Phys. Rev. Lett. 109 (2012) 094101]. DMSOmw 2013-07-10 15:16 © 2013 Arnaud Cuisset

Keywords: submillimeter spectrum, subTHz solid state spectrometer, rotational sideband, bending mode, accidental symmetric top, effective rotational Hamiltonian, gyroscopic destabilisation
PACS: 33.20.Sn, 33.15.Mt

1. Introduction

For about 50 years, dimethylsulfoxide $(CH_3)_2S{=}O$, or DMSO, was known as one of very few polyatomic asymmetric top molecules, whose moments of inertia $I_A \sim I_B \ll I_C$ are accidentally close to those of a symmetric top. However, it was not until 2012, that qualitative consequences of this exceptional situation were uncovered [1]. For nearly equal inertia moments $I_A \sim I_B$, the zero order rigid asymmetric rotor dynamics becomes vulnerable to higher order perturbations when the C-axis projection of the angular momentum $\boldsymbol{J}$ is small, i.e., when $|J_C| \ll J := \|\boldsymbol{J}\|$. Furthermore, when the centrifugal distortion forces become sufficiently strong, typically for large J, and also when these forces act in the "right direction", the rotational dynamics of the molecule may change qualitatively, and may exhibit "unusual" rotations, impossible in a rigid asymmetric Euler top. Analyzing the rotational structure of the vibrational state ν_{23} [1, 2] at 324 cm^{-1}, we have indeed found that for large J (the actual bifurcation happens for $J = 27.5$), the normally stable stationary rotation about the principal axis of inertia A becomes unstable, and two new equivalent axes of stationary rotation X emerge near A. For $J = 40 \ldots 50$, rotation about X becomes sufficiently stable, and four-fold degenerate quantum states (4-clusters or X-type states) appear at the high energy end of the rotational multiplet. Such localized states cannot occur in the case of a rigid top. At the same time, the rotational energy spectrum of both the ground state $|0\rangle$ and the vibrational state ν_{11} at 377 cm^{-1} [2, 3] does not present this anomaly, i.e., it remains qualitatively similar to that of the rigid top for all experimentally accessible $J < 70$.

The loss of stability of the stationary rotation about the principal axis A, that occurs in ν_{23} when J increases above ≈ 30, was called *gyroscopic destabilisation* [1]. Physical understanding of this phenomenon begins with determining whether it occurs due to a strong vibrational resonance with one or several close neighbor states, or the reasons lie deeper in the rotational dynamics of the specifically vibrating nonrigid molecule [2, Sec. IIIC.3]. In the former case, one should expect that the resonating state ν also has an unusual, strongly perturbed rotational structure. This structure can be obtained from the analysis of the far infrared (FIR) absorption spectrum $\nu_k \leftarrow 0$, and/or of the rotational sideband $\nu_k \leftarrow \nu_k$ in the microwave and submm-wave (MW)

*Corresponding author
Email addresses: arnaud.cuisset@univ-littoral.fr (Arnaud Cuisset), sadovski@univ-littoral.fr (Dmitrií A. Sadovskií)

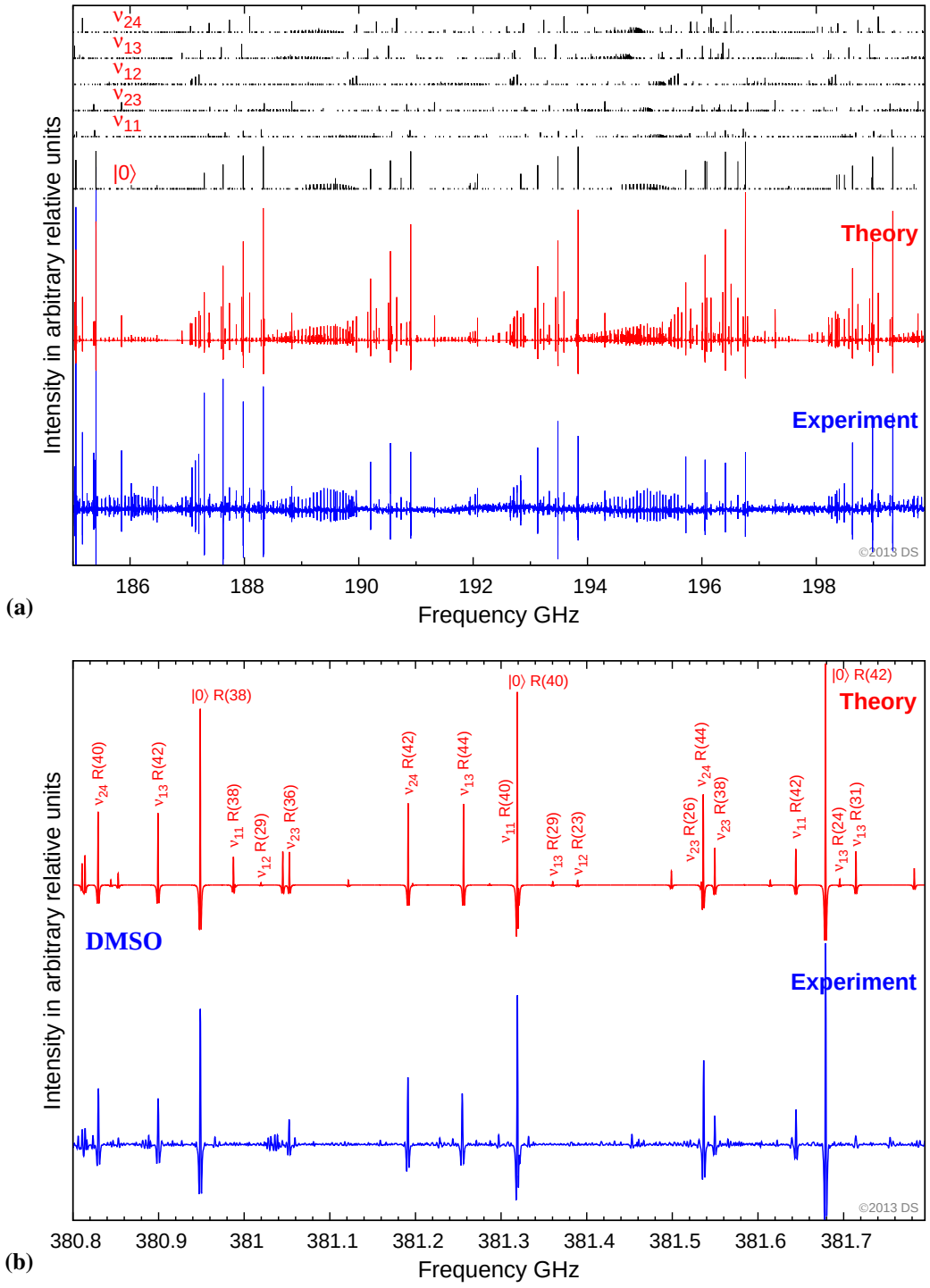

Figure 1: (a) 15 GHz (0.5 cm^{-1}) and (b) 1 GHz scans of the submm-wave absorption spectrum of DMSO. Upper (red) and lower (blue) traces show the experimental spectrum (sec. 2) and the simulated second derivative spectrum, respectively. The latter is calculated using the spectroscopic parameters in table 1 and the two-component permanent dipole moment (sec 3) Topmost stick diagrams in (a) represent calculated frequencies and relative intensities of the pure rotational transitions in the ground state and in the five lowest energy fundamental ($v = 1$) vibrational states.

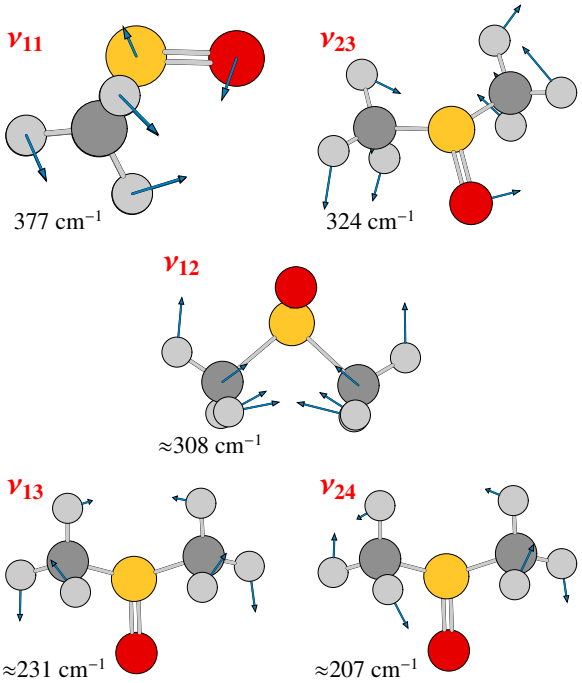

Figure 2: Five lowest frequency vibrational modes of DMSO computed with GAUSSIAN09 at the B3LYP/6-311+G(3df,2p) level of theory

spectrum. The FIR spectrum has the advantage of giving also the vibrational frequency of ν_k. On the other hand, the MW data are several orders of magnitude more accurate. Presently, only ν_{11} [3] and ν_{23} [1, 2] were uncovered in the FIR spectrum using contemporary techniques. So the MW spectrum comes to our rescue (fig. 1). Note that at room temperature, all states with energies up to about 400 cm^{-1} are sufficiently populated thermally to be observed as MW sidebands. When the methyl rocking modes ν_{13} and ν_{24} (fig. 2) get excited, the situation is somewhat complicated by the splitting of the rotational states due to the tunneling between different rocking minima. However, most of these splittings are small (less than 3 MHz) compared to typical spacings between the rotational lines, and can be ignored by taking average line positions. By doing so in the present work, we obtained rotational constants and centrifugal corrections to order J^8 of all fundamental vibrational states with energies below 400 cm^{-1}. We found that their rotational structure is "standard", i.e., similar to that of $|0\rangle$. This excludes the strong vibrational 1:1 resonance as a mechanism of the X-type state formation.

The precise information on the rotational constants and quartic centrifugal distortion parameters of DMSO in the ground state $|0\rangle$ was obtained first by Dreizler and Dendl in 1965 [4] from the MW spectrum in the 7–60 GHz frequency range. At the same time [5], it became also possible to assign a number of sideband MW transitions $\nu_k \leftarrow \nu_k$ involving the excited fundamental vibrational states of DMSO that correspond to the symmetric and asymmetric methyl rocking modes ν_{13} and ν_{24}, and the state ν_{12} representing the symmetric stretching of the SC_2 bonds (fig. 2). These three states lie below $\approx$ 300 cm^{-1}, and are practically invisible in the absorption spectrum $\nu_k \leftarrow 0$ because the corresponding vibrational modes do not alter significantly the dipole moment of the molecule. Further analysis in [6, 7] and later again in [8] focused on the geometry [9], the force field [10], and the tunneling splittings in the methyl rocking (aka internal rotation) states and the corresponding potential [5, 8]. Most recently, the ground state $|0\rangle$ to $J = 50$ has been re-analyzed in [11].

Until [1], the phenomenon of gyroscopic destabilization was known only for triatomic molecules AB_2 [12, 13, and references therein] with heavy central atom A and the bond angle slightly above 90°. Two types of 4-clusters, *rotational* and *vibrational*, were distinguished [12]. The rotational 4-clusters may be regarded as more complex dynamically and, therefore, more interesting. In the AB_2 molecules, rotational 4-clusters emerge at large J, when strong specific centrifugal forces decrease the bond angle and make it pass 90°, which corresponds to the exact symmetric top configuration [14]. Vibrational 4-clusters occur when two 1:1 resonant vibrations of AB_2 form a pair of stable equivalent nonlinear normal modes, such as the most familiar local modes [15, 16]. Then a 4-cluster is formed as a merger of two rotational doublets corresponding to the equivalent modes. The purpose of our present spectroscopic study of the rotational submm-wave sidebands of DMSO is to identify the most probable physical mechanism of the gyroscopic destabilization phenomenon in this polyatomic molecule [1, 2].

2. Experimental details

The solid state subTHz spectrometer used in the present study has been described in detail by Mouret *et al.* [17]. In this spectrometer, a post-amplified synthesizer (7.7 GHz - 12.2 GHz) drives a cascaded series of frequency multipliers, working at room temperature, to cover the frequency range between 50 and 930 GHz. At first, a Spacek active tripler is used to multiply the frequency of the synthesizer by 3 and amplify. The output power is high enough to use passive Schottky multipliers (×2, ×3) from Virginia Diodes Inc. Combining these multipliers, five bands associated with

the ×9, ×18, ×27, ×36, and ×54 harmonics have been scanned in order to obtain the high resolution spectra of DMSO ranging from 70 to 700 GHz. For such kind of work, our multiplier chain driven by the commercial microwave synthesizer has certain advantages in comparison to optoelectronic techniques, such as continuous-wave THz by photomixing [18, 19], because it is easily phase locked, frequency agile, relatively rapid, robust and compact. Thus we were able to record each band continuously at a rate of 5 GHz/hour using a time constant of 300 ms at the 100 kHz spectral resolution. Furthermore, both amplitude and frequency modulation are straightforward, and various detection schemes can be implemented. Although the source phase noise for the multiplication factor n increases by a factor of $20\log(n)$, the useful spectral purity of the order of few kHz is sufficient for the THz analysis of the absorption lines of DMSO in the Doppler regime, whose full width at half maximum is about 100 kHz.

In our setup, the polarised radiation emitted from a horn antenna was collimated by an off axis parabolic mirror and injected into a 1.25 m long stainless steel absorption cell with Teflon windows. A second off-axis parabolic mirror focused the sub-THz beam at the entrance of the detector, an InSb liquid He-cooled bolometer from QMC Instruments. In order to improve the sensitivity, the sources were frequency modulated at 50 kHz and lock-in detection with the second harmonic was used. DMSO with purity better than 97% from Aldrich Chemical Co. was used without further purification. The cell was filled by direct injection of the saturated vapor pressure at room temperature. The typical working gas pressure, monitored by a capacitor gauge with the range of $10^4 \ldots 10^1$ mbar, was 20 μbar.

Figures 1(a) and 1(b), show parts of the experimental spectrum of DMSO in the 180 GHz and 380 GHz regions, respectively. We obtained signal-to-noise (S/N) ratios better than 20 for both the $0 \leftarrow 0$ transitions in the ground state, and the $\nu_k \leftarrow \nu_k$ sideband transitions in the excited vibrational states. Taking into account the S/N ratio and the linewidths, the precision on the measured frequencies was better than 30 kHz for the most intense transitions.

3. Analysis of the spectrum

The combined data used in our present analysis consisted of about 3000 $0 \leftarrow 0$ transitions reported in [11], and about 80 $\nu_k \leftarrow \nu_k$ sideband transitions with $\nu_k = \nu_{12}$, ν_{13}, and ν_{24} assigned initially by Dreizler and Dendl [5] in the 5–54 GHz MW domain, to which we added about 4000 newly assigned transitions in our submm-wave spectrum. The latter included about 700 additional $0 \leftarrow 0$ transitions, and 500–600 transitions in each sideband with J values up to 60. For ν_{11} and ν_{23}, we also used our FIR data from [2] with weights reflecting their lower accuracy. The initial rotational Hamiltonian $H_{\rm rot}$, that was used to start the assignment of the new transitions, was set up as follows. The ground state parameters of $H_{\rm rot}$ were based on [11]; we already used them before in [1–3]. The parameters of ν_{11} and ν_{23} to order J^6 were obtained in [2]. The basic parameters of ν_{12}, ν_{13}, and ν_{24} to order J^4 were fitted to the transitions in [5]. This set of parameters allowed many new unambiguous assignments with subsequent iterative refinements using the SPFIT/SPCAT programs [20, 21]. Standard Loomis-Wood techniques [22] helped speeding up further assignments.

With notable exception of ν_{12}, our accuracy of reproducing the assigned sideband transitions was about 1.2–1.5 MHz, about 20 times worse than that for the principal $0 \leftarrow 0$ band. We can give several reasons for this: our data lie at higher frequencies where the spectral accuracy is lower; the sideband transitions are at least two orders of magnitude weaker than the ground state transitions and, subsequently are more affected by noise and strong neighbors; we had to compromise on weeding out weak and blended sideband transitions in order to obtain more complete data sets. For the latter reason, we kept using in the fit a number of the $\nu_{12} \leftarrow \nu_{12}$ transitions near $J = 35 \ldots 40$ with a clear strong level crossing pattern. This gave a notably higher fit error of 10 MHz for ν_{12}.

Our resulting final parameters are given in table 1; a complet set of parameters, and the list of all fitted transitions are provided in electronic format (Appendix A). Figure 3 shows the part of the rotational multiplet of ν_{12}, ν_{13}, and ν_{24}, that we observed and assigned successfully in this work. It is large enough to uncover the whole rotational structure up to $J \approx 50$. The information on these states comes solely from our submm-wave data and is of primary interest in our context.

A quantitative study of intensities was beyond our purpose. To reproduce the intensities of all $\nu_k \leftarrow \nu_k$ transitions qualitatively, we used a simple permanent dipole moment function. The permanent dipole moment $\boldsymbol{\mu}$ of DMSO lies in the symmetry plane BC and has one essential adjustable parameter μ_B/μ_C. Furthermore, $\boldsymbol{\mu}$ is nearly parallel to the S−O bond, and a good estimate for $\mu_c/\mu_b = 0.38$ can be given using Gaussian predictions of both equilibrium positions and effective charges on each atom.

We should mention several problems that we have en-

Table 1: Vibration-rotation parameters (MHz) of the effective Hamiltonian of DMSO in the model of isolated vibrational states; the value of a parameter for the vibrational state ν_k equals the sum of values in columns $|0\rangle$ and ν_k, e.g., $A_{|\nu_k\rangle} = A + \delta_k A$; the asterisk $*$ marks fixed values

Parameter	$\|0\rangle$	ν_{11}	ν_{23}	ν_{12}	ν_{13}	ν_{24}	Units
$\omega \times 10^{-6}$	0*	11.294718152(102)	9.712918222(86)	9.2336077064*	6.9252057798*	6.2057038806*	THz
A	7036.5822165(234)	5.00827(38)	0.87042(32)	23.97618(71)	1.21688(74)	−6.67641(54)	MHz
B	6910.8301279(228)	3.58947(35)	−6.869466(309)	−13.59240(71)	−31.78370(69)	−11.57229(52)	MHz
C	4218.776511(44)	−1.03729(63)	11.97226(49)	−27.39443(88)	−8.24675(76)	−5.34677(62)	MHz
$-D_K \times 10^3$	−3.989536(48)	0.18961(135)	−0.40758(91)	1.52607(151)	−0.57739(113)	0.08309(85)	kHz
$-D_{JK} \times 10^3$	8.938057(49)	−0.43457(122)	0.58693(89)	−0.15445(169)	0.43850(119)	−0.16506(94)	kHz
$-D_J \times 10^3$	−6.0889172(164)	0.33021(38)	−0.494682(311)	1.32624(74)	−0.13384(59)	0.07190(42)	kHz
$d_1 \times 10^3$	−0.1639913(103)	0.062048(182)	3.816647(169)	0.24689(61)	0.24458(71)	−0.10379(49)	kHz
$d_2 \times 10^3$	−0.2717076(58)	0.029928(100)	−7.220041(77)	−0.02509(34)	−0.42752(35)	−0.02200(32)	kHz
$H_K \times 10^6$	−0.0219640(256)	−0.00780(133)	0.09023(85)	−1.10825(149)	−0.55172(103)	0.06710(56)	Hz
$H_{JKK} \times 10^6$	0.052778(37)	−0.04461(171)	−0.30670(107)	−0.37143(223)	1.84694(151)	−0.15744(86)	Hz
$H_{JJK} \times 10^6$	−0.0396809(242)	0.12680(104)	0.04014(68)	0.15979(155)	−1.59441(115)	0.13936(73)	Hz
$H_J \times 10^6$	0.0088016(81)	−0.076845(299)	0.105985(221)	−1.45498(59)	0.43361(52)	−0.043980(303)	Hz
$h_1 \times 10^6$	−0.0017637(63)	−0.014422(112)	−0.510122(100)	−0.11616(40)	−0.12145(57)	0.19330(37)	Hz
$h_2 \times 10^6$	0.0010658(51)	−0.001472(88)	1.287893(98)	0.000671(316)	1.03593(39)	−0.31322(33)	Hz
$h_3 \times 10^6$	−0.00137384(224)	−0.003101(44)	1.882887(43)	−0.003347(83)	−0.090598(111)	0.023808(52)	Hz
$L_K \times 10^9$	−0.0001187(60)	0.16748(68)	−0.21012(42)	−0.21140(82)	0.08953(85)	−0.11828(39)	mHz
$L_{KKJ} \times 10^9$	0.0004250(116)	−0.33892(111)	0.46541(65)	1.28923(168)	−0.00120(205)	0.28849(98)	mHz
$L_{JK} \times 10^9$	−0.0004380(104)	0.24142(84)	−0.23194(49)	−1.04284(158)	−0.42420(186)	−0.24914(96)	mHz
$L_{JJK} \times 10^9$	0.0001788(57)	−0.09700(45)	0.003583(273)	0.40264(79)	0.43358(96)	0.09011(46)	mHz
$L_J \times 10^9$	−0.00000241(174)	0.018924(117)	0.000978(87)	0.499561(215)	−0.119384(277)	−0.012330(105)	mHz
$l_1 \times 10^{12}$	0.03155(181)	5.7287(266)	−9.4031(216)	0.0534(85)	0.0452(85)	0.0454(85)	μHz
$l_2 \times 10^{12}$	−0.02414(161)	3.0923(253)	−61.9827(292)	0.0197(82)	−0.0077(82)	−0.0031(82)	μHz
$l_3 \times 10^{12}$	0.01604(92)	3.1722(174)	2.6091(147)	0.0474(37)	0.0441(37)	0.0340(37)	μHz
$l_4 \times 10^{12}$	0*	1.1625(60)	0.5563(41)	0*	0*	0*	μHz

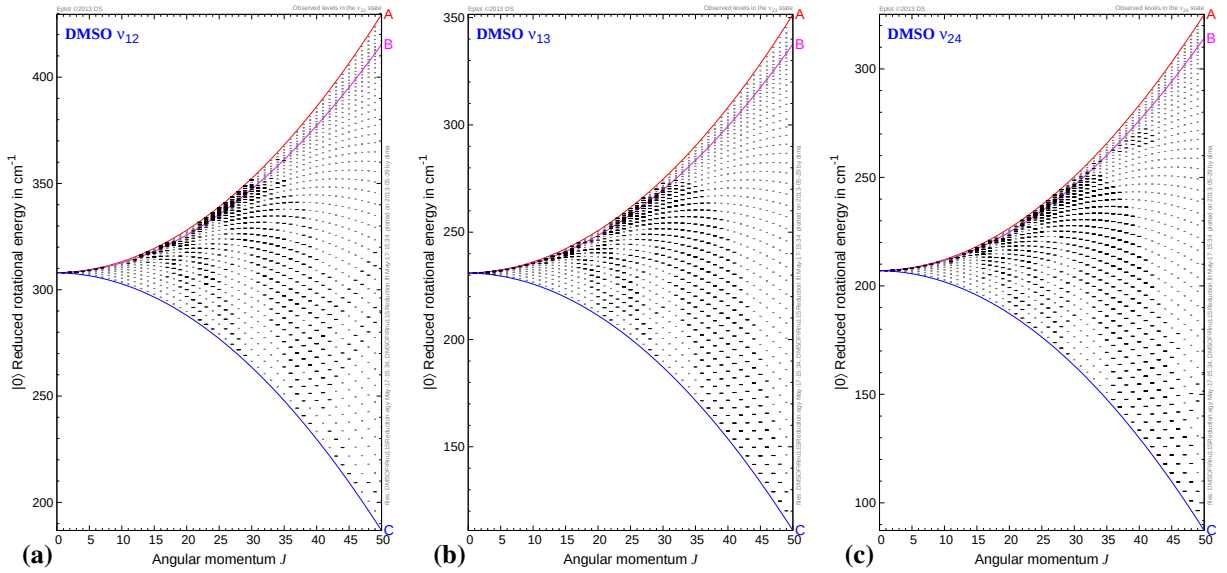

Figure 3: Rotational structure of the low frequency vibrational states of DMSO reconstructed using parameters in Table 1. Energies (level dashes) are shown after subtracting the average classical ground state rotational energy $(\mathcal{H}^0_A(J) + \mathcal{H}^0_C(J))/2$; observed levels are marked by longer dashes; bold solid lines represent energies of classical rotation about stationary axes (relative equilibria).

countered and that remain to be resolved. In ν_{13} and ν_{24}, we ignored the splittings due to tunneling between different methyl rocking equilibria with estimated internal rotation barrier of about 1000 cm^{-1}according to our Gaussian calculation and [8]. This fine structure was not important to our search for potential perturbers of ν_{23}, but it can clearly be studied using our data. Furthermore, we observed one or several double excited rocking states. Their analysis is of interest both to our purpose, and to the study of rocking dynamics. And finally, the strong level crossings—the last but not the least, that we saw in ν_{11} and especially ν_{12}, call for reconciling with the known/estimated vibrational energies and for the eventual assignments pending further analysis of the rocking states.

4. Rotational structure

The scale of the total splitting of the rotational multiplet of DMSO (approximately 250 cm^{-1} for $J = 50$, cf Fig. 3) does not allow to assess directly the differences in the rotational structure of different vibrational states. To understand these differences, for each vibrational state ν_k, and for each principal axis of inertia $s = A, B, C$, we consider classical energy

$$\mathcal{H}^{\nu_k,s}(J) = \left(H_{\rm rot}^{\nu_k,s}(J) - \omega_{\nu_k} - H_{\rm rot}^{0,s}(J)\right) / \left(J(J+1)\right)$$

of stationary rotation about s relative to the energy of such rotation in the ground state $|0\rangle$ and factored by $J(J+1)$. The limit of $\mathcal{H}^{\nu_k,s}(J)$ for $J \to 0$ is the difference δs between the inverse moment of inertia $1/(2I_s)$ in the excited state ν_k and $|0\rangle$. This difference reflects the change of the averaged geometry of the molecule. With increasing J, as long as the rotation about s and the particular vibration ν_k are well separated, i.e., vibration remains much "faster", we should expect $\mathcal{H}^{\nu_k,s}(J)$ to vary but insignificantly compared to the value of δs. On the other hand, large variation of $\mathcal{H}^{\nu_k,s}(J)$ signals essential vibration-rotation interactions, and significant perturbations in the rotational level system.

Figure 4 shows graphs of functions $\mathcal{H}^{\nu_k,s}(J)$ for fundamental vibrational states ν_{11}, ν_{23}, ν_{12}, ν_{13}, and ν_{24} of DMSO. We can see that in most cases—except for $\mathcal{H}^{\nu_{23},A}(J)$, these functions behave as we anticipated: nearly constant at low J, and some varying notably above $J = 25$. The *only* exceptional function $\mathcal{H}^{\nu_{23},A}(J)$ presents a qualitatively different, strong, immediate nonlinear variation at low J. From the explicit expression for $\mathcal{H}^{\nu_{23},A}(J)$ with $j = \sqrt{J(J+1)}$

$$\mathcal{H}^{\nu_{23},A}(J) = \delta A - (\delta D_J - 2(\delta d_1 - \delta d_2))\, j^2 + O(j^4),$$

we can see that the formal reason for this behavior of $\mathcal{H}^{\nu_{23},A}(J)$ is in the anomalously large tensorial corrections of order J^4 with phenomenological parameters d_1 and d_2. Turning to the physical explanation, we can think of the breakdown of the rotation-vibration separation in the case of the excited ν_{23} vibration and rotation about axis A which results in such corrections.

Another quantity that can help visualizing the exceptional properties of ν_{23} is the dynamic asymmetry

$$\varepsilon(J) = \sqrt{\frac{H_{\rm rot}^{A}(J) - H_{\rm rot}^{B}(J)}{H_{\rm rot}^{A}(J) - H_{\rm rot}^{C}(J)}},$$

whose graph is also presented in fig. 4. In the limit of $J \to 0$, this quantity gives the static asymmetry[1] of the top. In different excited vibrational states, the molecule has different averaged geometry, and, consequently, different asymmetry ε. The latter remains nearly constant as long as vibration and rotation remain separated. Thus we see that DMSO becomes more asymmetric in the states ν_{12} and ν_{13}, than in ν_{11}, ν_{24}, and $|0\rangle$. Again we see an exceptional behavior in the ν_{23} state, where ε drops quickly and immediately with J, and the molecule approaches the symmetric top configuration.

5. Conclusions and questions

Within the model of an isolated vibrational state, the rotational multiplet of ν_{23} can only be described using anomalously large tensorial corrections of orders J^4 and higher, see [1, 2] and table 1. Generally, this signifies strong rotation-vibration interactions. One possibility for such global perturbation of ν_{23} may be the coupling with one (or several) neighbor state(s) via a wide 1:1 resonance and the Coriolis interaction of type qpJ. For this to happen, the perturber(s) should lie within 5–10 cm^{-1} of ν_{23}. Unfortunately, except for that of ν_{11}, other low vibrational frequencies of DMSO are poorly known; their estimates vary.

In our present work, we have found that all other low energy fundamental vibrational states of DMSO have standard, relatively unperturbed rotational structure, similar to that in the ground state $|0\rangle$. Therefore, none of these states can be at the origin of the interactions distorting ν_{23}, and the possibility for the 1:1 resonance to play a decisive role in the rotational dynamics of ν_{23} appears highly unlikely.

So, with the simplest possibility thus excluded, what can be the next most likely scenario? We have still to

[1] Spectroscopists also often use $\kappa = 1 - 2\varepsilon^2$

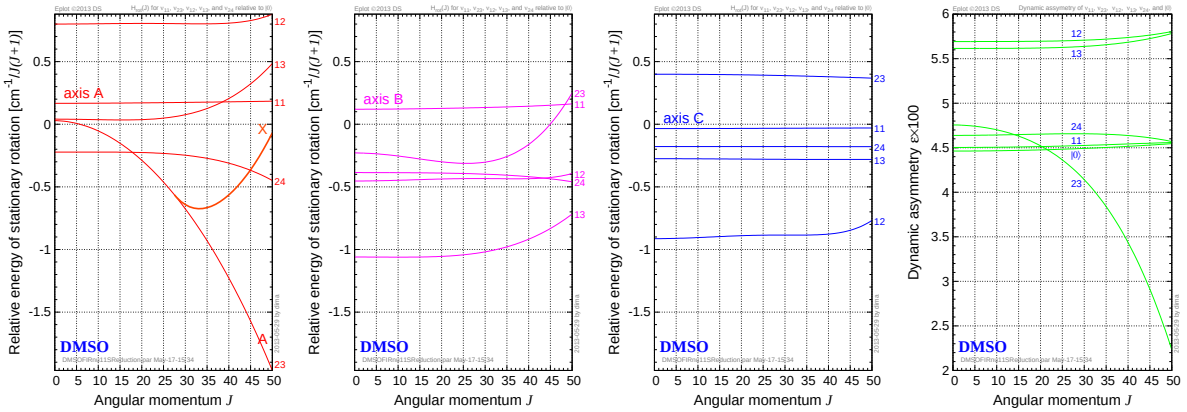

Figure 4: Energy of classical stationary rotation about principal inertia axes A, B, and C relative to that in the ground state $|0\rangle$ and factored by $J(J+1)$, and dynamic asymmetry for fundamental vibrational states ν_{11}, ν_{23}, ν_{12}, ν_{13}, and ν_{24} of DMSO reconstructed using parameters in Table 1.

examine the overtones $2\nu_{13}$, $2\nu_{24}$, and the combination state $\nu_{13}+\nu_{24}$ of the rocking modes, one of which may come close to ν_{23} and engage the latter through a 1:2 resonance and high order Coriolis couplings. These interactions, however, are much narrower in comparison to the 1:1 resonance, and are more likely to result in avoided-crossing-type perturbations, than in the global distortion of the upper part of the multiplet, that we observe in ν_{23}. Note that no such crossings have been observed so far, and that the information on the double excited rocking states can be extracted from our submm-wave spectrum.

On the other hand, if the reasons are to be sought for, eventually, in the classical rotational dynamics proper of the vibrating DMSO molecule in the ν_{23} state, it seems that a lead to follow maybe the symmetry of ν_{23}, and the fact that the perturbation affects only the upper part of the multiplet, i.e., rotations about axis A. An attempt to accommodate for these two circumstances within the framework of a classical Howard–Wilson rotation-vibration Hamiltonian seems to be the most appropriate direction to explore.

Acknowledgments

We thank Michael Klemm and Tamina Greifeld from the Verlag der Zeitschrift für Naturforschung for providing us timely with the reprints by Dreizler and Dendl [4, 5], which were instrumental at the beginning of our analysis.

Appendix A. Supplementary materials

The parameters of all fundamental vibrational states of DMSO studied in this paper, and the list of the assigned spectroscopic transitions can be found in the Pickett's [20] `.par` and `.lin` formats, respectively, as supplementary data associated with this article in the online version at doi:10.1016/j.cplett.2013.??.???.

References

[1] A. Cuisset, O. Pirali, and D.A. Sadovskií, Phys. Rev. Lett. 109 (2012) 094101/1.
[2] A. Cuisset and D.A. Sadovskií, J. Chem. Phys. 138 (2013) 234302/1.
[3] A. Cuisset, L. Nanobashvili, I. Smirnova, R. Bocquet, F. Hindle, G. Mouret, O. Pirali, P. Roy, and D.A. Sadovskií, Chem. Phys. Lett. 492 (2010) 30.
[4] H. Dreizler and G. Dendl, Z. Naturforsch. 20a (1965) 30.
[5] H. Dreizler and G. Dendl, Z. Naturforsch. 20a (1965) 1431.
[6] W. Feder, H. Dreizler, H.D. Rudolph, and V. Typke, Z. Naturforsch. A 24 (1969) 266.
[7] V. Typke, J. Mol. Spectrosc. 63 (1976) 170, see Table II on p. 174 for mw data on DMSO.
[8] E. Fliege, H. Dreizler, and V. Typke, Z. Naturforsch. A 38 (1983) 668.
[9] V. Typke, J. Mol. Struct. 384 (1996) 35.
[10] V. Typke and M. Dakkouri, J. Mol. Struct. 599 (2001) 177.
[11] L. Margulès, R.A. Motiyenko, E.A. Alekseev, and J. Demaison, J. Mol. Spectrosc. 260 (2010) 23.
[12] I.N. Kozin and P. Jensen, J. Mol. Spectrosc. 161 (1993) 186.
[13] I.N. Kozin and I.M. Pavlichenkov, J. Chem. Phys. 104 (1996) 4105.
[14] I.M. Pavlichenkov and B.I. Zhilinskií, Ann. Phys. (N.Y.) 184 (1988) 1.
[15] I.N. Kozin, D.A. Sadovskii, and B.I. Zhilinskii, Spectrochim. Acta A 61 (2005) 2867.
[16] H. Crogman, V. Boudon, and D.A. Sadovskii, Europ. Phys. J. D 42 (2007) 61.
[17] G. Mouret, M. Guinet, A. Cuisset, L. Croize, S. Eliet, R. Bocquet, and F. Hindle, IEEE Sensors J. 13 (2013) 133.
[18] F. Hindle, C. Yang, G. Mouret, A. Cuisset, R. Bocquet, J.F. Lampin, K. Blary, E. Peytavit, T. Akalin, and G. Ducournau, IEEE Sensors J. 9 (2009) 9039.
[19] F. Hindle, G. Mouret, S. Eliet, M. Guinet, A. Cuisset, R. Bocquet, T. Yasui, and D. Rovera, Appl. Phys. B 104 (2011) 763.

[20] H.M. Pickett, "SPFIT/SPCAT programs for vibration-rotation spectra," (2007), for more information and examples see also http://www.ph1.uni-koeln.de/cdms/pickett and http://info.ifpan.edu.pl/~kisiel/asym/pickett/crib.htm.
[21] H.M. Pickett, J. Mol. Spectrosc. 148 (1991) 371.
[22] W. Lodyga, M. Kreglewski, P. Pracna, and S. Urban, J. Mol. Spectrosc. 243 (2007) 182.